Supporting Information

Reactive Flux Assisted Metal Oxide-Boron-Sulfur Routine for Syntheses of $CsRESiS_4$ (RE = Sm, Gd−Ho): Featuring Nonlinear Optical Activity and Wide Band Gaps

Zhen-Cheng Wu,[a#] Fang-Xu Tian,[a#] Rui Xiao,[a] Mao-Yin Ran,[a] Wenlong Liu,[c] Wen-Tong Chen,[b*] Sheng-Ping Guo[a*]

[a]Yunnan Key Laboratory of Electromagnetic Materials and Devices, School of Materials and Energy, Yunnan University, Kunming 650500, P. R. China

[b]School of Chemistry and Chemical Engineering, Key Laboratory of Jiangxi Province for Special Optoelectronic Artificial Crystal Materials, Ji'an Key Laboratory of Photoelectric Crystal Materials and Device, Humic Acid Utilization Engineering Research Center of Jiangxi Province, Jinggangshan University, Ji'an, Jiangxi 343009, P. R. China

[c]School of Chemistry and Chemical Engineering, Yangzhou University, Yangzhou, Jiangsu 225002, P. R. China

*E-mail: 9920060002@jgsu.edu.cn; spguo@ynu.edu.cn

Contents

Table S1 Crystal data and structure refinement parameters for **1** and **4.**

Chemical formula	$CsSmSiS_4$(**1**)	$CsDySiS_4$(**4**)
Formula weight (g mol^{-1})	439.59	451.74
Temperature (K)	296	
Crystal system	orthorhombic	
Space group	$P2_12_12_1$	
a (Å)	6.3858(5)	6.3429(5)
b (Å)	6.7122(6)	6.6737(5)
c (Å)	17.709(15)	17.6177(14)
V ($Å^3$)	759.06(11)	747.19(8)
Z	4	
D_{calc} (g/cm^3)	3.847	4.016
μ (mm^{-1})	13.605	15.963
F (000)	780	796
2θ range (°)	4.600 to 50.018	6.526 to 50.007
GOF on F^2	1.072	1.131
Flack parameter	0.35(3)	0.35(3)
Final *R* indexes [I ≥ 2σ (I)]	R_1 = 0.0225, wR_2 = 0.0539	R_1 = 0.0271, wR_2 = 0.0508
Final *R* indexes [all data]	R_1 = 0.0240, wR_2 = 0.0545	R_1 = 0.0304, wR_2 = 0.0515
Largest diff. peak/hole/e $Å^{-3}$	1.931/-1.409	1.764/-1.266

[a] $R_1 = \Sigma||F_o| - |F_c||/\Sigma|F_o|$ and $wR_2 = [\Sigma w(F_o^2 - F_c^2)^2/\ \Sigma wF_o^4]^{1/2}$ for ($Fo^2 > 2\sigma\ (Fo^2)$)

Table S2 The structural parameters obtained after refinement across the **1**–**5**.

Sample	Phase	*a* (Å)	*b* (Å)	*c* (Å)	*V* (Å^3)	R_{wp}	χ^2
Sm	$P2_12_12_1$	6.38676	6.70560	17.70869	758.412	11.4	1.32
Gd	$P2_12_12_1$	6.36538	6.68922	17.67177	752.454	10.3	1.35
Tb	$P2_12_12_1$	6.34314	6.67700	17.65926	747.925	12.1	1.75
Dy	$P2_12_12_1$	6.32551	6.66739	17.63567	743.778	9.69	1.32
Ho	$P2_12_12_1$	6.32513	6.65650	17.61571	741.678	11.9	2.29

Table S3 Atomic coordinates (× 10^4) and equivalent isotropic displacement parameters (U_{eq}, Å^2 × 10^3) for **1** and **4**. U_{eq} is defined as one third of the trace of the orthogonalized U_{ij} tensor.

Atom	*Wyck.*	*x*	*y*	*z*	U_{eq}
			1		
Sm(1)	4*a*	7075(1)	5182(1)	2281(1)	20(1)
Cs(2)	4*a*	29(1)	4922(1)	4674(1)	40(1)
S(3)	4*a*	3948(5)	7468(3)	1525(2)	21(1)
S(4)	4*a*	4281(5)	2506(3)	1443(2)	21(1)
S(5)	4*a*	-513(3)	4873(5)	944(1)	23(1)
S(6)	4*a*	1180(4)	4383(4)	2787(1)	23(1)
Si(7)	4*a*	2107(4)	4840(4)	1650(1)	19(1)
			4		
Dy(1)	4*a*	7923(1)	5191(1)	2282(1)	14(1)
Cs(2)	4*a*	4956(2)	4918(2)	4678(1)	31(1)
S(3)	4*a*	1050(7)	7463(4)	1543(2)	12(1)
S(4)	4*a*	699(7)	2501(4)	1454(2)	12(1)
S(5)	4*a*	3871(5)	4333(4)	2794(2)	15(1)
S(6)	4*a*	5537(4)	4877(5)	952(2)	14(1)
Si(7)	4*a*	2896(5)	4833(5)	1662(2)	11(1)

Table S4 Bond lengths (Å) and bond angle for **1** and **4**.

		1	
Sm(1)-S(3)#3	2.866(3)	Cs(2)-S(5)#8	3.660(2)
Sm(1)-S(3)	2.852(3)	Cs(2)-S(5)#6	4.164(2)
Sm(1)-S(4)#4	2.879(3)	Cs(2)-S(6)	3.441(3)
Sm(1)-S(4)	2.934(3)	Si(7)-S(3)	2.132(4)
Sm(1)-S(5)#1	2.832(2)	Si(7)-S(4)	2.125(4)
Sm(1)-S(6)#1	2.821(2)	Si(7)-S(5)	2.089(3)
Sm(1)-S(6)#4	3.035(2)	Si(7)-S(6)	2.120(3)
Cs(2)-S(3)#5	3.698(3)	S(4)-Si(7)-S(3)	103.40(13)
Cs(2)-S(3)#6	3.708(3)	S(5)-Si(7)-S(3)	111.77(17)
Cs(2)-S(4)#6	3.605(3)	S(5)-Si(7)-S(4)	115.33(16)
Cs(2)-S(4)#7	3.808(3)	S(5)-Si(7)-S(6)	110.26(13)
Cs(2)-S(5)#7	3.513(3)	S(6)-Si(7)-S(3)	111.86(15)
Cs(2)-S(5)#5	3.574(3)	S(6)-Si(7)-S(4)	103.86(15)
		4	
Dy(1)-S(3)#2	2.835(3)	Cs(2)-S(6)#6	3.660(2)
Dy(1)-S(3)#3	2.817(4)	Cs(2)-S(6)#5	4.148(3)
Dy(1)-S(4)#3	2.907(3)	Cs(2)-S(6)#4	3.505(4)
Dy(1)-S(4)#4	2.849(3)	Si(7)-S(3)	2.120(5)
Dy(1)-S(5)	2.784(3)	Si(7)-S(4)	2.121(5)
Dy(1)-S(5)#4	2.992(3)	Si(7)-S(5)	2.117(4)
Dy(1)-S(6)	2.801(3)	Si(7)-S(6)	2.093(4)
Cs(2)-S(3)#5	3.711(3)	S(3)-Si(7)-S(4)	103.40(13)
Cs(2)-S(3)#2	3.708(4)	S(5)-Si(7)-S(3)	112.65(18)
Cs(2)-S(4)#5	3.601(3)	S(5)-Si(7)-S(4)	103.83(18)
Cs(2)-S(4)#4	3.816(4)	S(6)-Si(7)-S(3)	111.8(2)
Cs(2)-S(5)	3.420(3)	S(6)-Si(7)-S(4)	115.65(19)
Cs(2)-S(6)#2	3.557(4)	S(6)-Si(7)-S(5)	109.48(18)

Symmetry transformations used to generate equivalent atoms:

#1 -x+3/2,-y+1,z-1/2 #2 -x+1,y-1/2,-z+1/2 #3 x+1,y,z

#4 -x+1,y+1/2,-z+1/2 #5 -x+1/2,-y+1,z+1/2 #6 -x+3/2,-y+1,z+1/2

#7 x-1,y,z #8 -x+1/2,-y+1,z-1/2

Table S5 Bond valence sum (BVS) calculation results for **1**−**5**.

1		**2**		**3**		**4**		**5**	
Atom	**BVS**	**Atom**	**BVS**	**Atom**	**BVS**	**Atom**	**BVS**	**Atom**	**BVS**
Sm(1)	2.78	Gd(1)	2.88	Tb(1)	2.7	Dy(1)	2.86	Ho(1)	2.79
Cs(1)	1.17	Cs(1)	1.17	Cs(1)	1.17	Cs(1)	1.18	Cs(1)	1.17
Si(1)	4.12	Si(1)	4.13	Si(1)	4.1	Si(1)	4.11	Si(1)	4.17
S(1)	2.06	S(1)	2.02	S(1)	2.01	S(1)	1.91	S(1)	1.97
S(2)	2.01	S(2)	2.1	S(2)	1.96	S(2)	2.01	S(2)	1.93
S(3)	2.03	S(3)	2.05	S(3)	2.01	S(3)	2.04	S(3)	1.98
S(4)	1.98	S(4)	2.02	S(4)	1.98	S(4)	2	S(4)	1.94

Table S6 Summary of reported ternary/quaternary rare-earth chalcogenides with noncentrosymmetric structures.

Number	Compound	Symmetry	Motifs	E_g (eV)	Reference
1	YBa_2GaTe_5	$Cmc2_1$	$[YTe_6]+[BaSe_8]+[GaTe_4]$	1.08	1
2	La_3BeSbS_7	$P6_3$	$[LaS_8]+[BeS_4]+[SbS_6]$	1.27	2
3	$YAgTe_2$	$P\bar{4}2_1m$	$[YTe_6]+[AgTe_4]$	1.37	3
4	$La_6Pb_3Si_2S_{14}$	$R\bar{3}c$	$[LaS_8]+[SiS_4]$	1.41	4
5	Sc_3InS_6	$P2_12_12_1$	$[ScS_8]+[YS_7]+[InS_4]+[InS_6]$	1.44	5
6	Y_3InS_6	$P2_12_12_1$	$[YS_8]+[YS_7]+[InS_4]+[InS_6]$	1.50	5
7	$Gd_2Sr_3Sn_3S_{12}$	$Pmc2_1$	$[GdS_8]+[SnS_4]$	1.51	6
8	La_3InS_6	$P2_12_12_1$	$[LaS_8]+[LaS_7]+[InS_4]+[InS_6]$	1.54	4
9	$Gd_2Ca_3Sn_3S_{12}$	$P\bar{6}_2m$	$[GdS_8]+[SnS_4]$	1.63	5
10	$ScAgSe_2$	$P2_12_12_1$	$[ScSe6]+[AgSe_4]$	1.64	7
11	$La_2Ca_3Sn_3S_{12}$	$P\bar{6}_2m$	$[LaS_8]+[SnS_4]$	1.65	5
12	$Sm_2Ca_3Sn_3S_{12}$	$P\bar{6}_2m$	$[SmS_8]+[SnS_4]$	1.66	5
13	$La_2Sr_3Sn_3S_{12}$	$Pmc2_1$	$[LaS_8]+[SnS_4]$	1.68	5
14	$Sm_6MnGe_2S_{14}$	$P6_3$	$[SmS_8]+[MnS_6]+[GeS_4]$	1.69	8
15	$Sm_2Sr_3Sn_3S_{12}$	$Pmc2_1$	$[SmS_8]+[SnS_4]$	1.71	5
16	$YAgSe_2$	$P2_12_12_1$	$[YSe_6]+[AgSe_4]$	1.75	6
17	$ScCuS_2$	$P3m1$	$[ScS_6]+[CuS_4]$	1.80	9
18	$La_3Sb_{0.33}SiS_7$	$P6_3$	$[LaS_8]+[SbS_6]+[SiS_4]$	1.92	10
19	$KSmP_2Se_6$	$P2_1$	$[SmSe_7]+[P_2Se_6]$	1.92	11
20	$La_3CuSiSe_7$	$P6_3$	$[LaSe_8]+[CuSe_3]+[SiSe_4]$	1.96	12
21	$La_3AgSiSe_7$	$P6_3$	$[LaSe_8]+[AgSe_3]+[SiSe_4]$	1.97	12
22	$EuHgGeSe_4$	$Ama2$	$[EuSe_8]+[HgSe_4]+[GeSe_4]$	1.97	13
23	$Y_3CuSiSe_7$	$P6_3$	$[YSe_7]+[CuSe_3]+[SiSe_4]$	1.99	14
24	$Ce_8Sb_2S_{15}$	$I4_1cd$	$[CeS_8]+[CeS_7]+[SbS_3]$	1.99	15
25	$La_3CuSnSe_7$	$P6_3$	$[LaSe_8]+[CuSe_3]+[SnSe_4]$	2.01	16
26	$EuHgGeS_4$	$Ama2$	$[EuS_8]+[HgS_4]+[GeS_4]$	2.04	17
27	La_2CuSbS_5	$Ima2$	$[LaS_8]+[LaS_{10}]+[CuS_4]+[SbS_4]$	2.06	18
28	La_4InSbS_9	$P4_12_12$	$[LaS_6]+[InS_4]+[SbS_4]$	2.07	19
29	$La_3AgSnSe_7$	$P6_3$	$[LaSe_8]+ [AgSe_3]+[SnSe_4]$	2.10	20
30	Y_3CuGeS_7	$P6_3$	$[YS_7]+[CuS_3]+[GeS_4]$	2.12	21
31	Sm_4InSbS_9	$P4_32_12$	$[SmS_6]+[InS_4]+[SbS_4]$	2.13	22
32	La_3BeBiS_7	$P6_3$	$[LaS_8]+[BeS_4]+[BiS_6]$	2.14	2

33	La_3CuSiS_7	*P*6$_3$	[LaS_8]+[CuS_3]+[SiS_4]	2.14	23
34	$EuHgSnS_4$	*Ama*2	[$EuSe_8$]+[$HgSe_4$]+[$GeSe_4$]	2.14	13
35	$Y_3CuGeSe_7$	*P*6$_3$	[YSe_7]+[$CuSe_3$]+[$GeSe_4$]	2.21	24
36	$La_6MnGe_2S_{14}$	*P*6$_3$	[LaS_8]+[MnS_6]+[GeS_4]	2.22	8
37	Sm_4GaSbS_9	*Aba*2	[SmS_7]+[SmS_6]+[GaS_4]+[SbS_4]	2.23	3325
38	$EuCdGeSe_4$	*Ama*2	[$EuSe_8$]+[$CdSe_4$]+[$GeSe_4$]	2.25	26
39	Y_3CuSiS_7	*P*6$_3$	[YS_8]+[CuS_3]+[SiS_4]	2.28	2214
40	Sm_3CuGeS_7	*P*6$_3$	[SmS_7]+[CuS_3]+[GeS_4]	2.29	27
41	$Eu_2Ga_2GeS_7$	*P*$\bar{4}$2$_1$*m*	[EuS_6]+[GaS_4]+[GeS_4]	2.30	28
42	$La_8Sb_2S_{15}$	*I*4$_1$*cd*	[CeS_8]+[CeS_7]+[SbS_3]	2.30	29
43	YBa_2InSe_5	*Cmc*2$_1$	[YSe_6]+[$BaSe_8$]+[$InSe_4$]	2.31	30
44	La_3CuSnS_7	*P*6$_3$	[LaS_8]+[CuS_3]+[SnS_4]	2.32	31
45	La_3AgSiS_7	*P*6$_3$	[LaS_8]+[AgS_3]+[SiS_4]	2.34	32
46	La_3AgGeS_7	*P*6$_3$	[LaS_8]+[AgS_3]+[GeS_4]	2.38	33
47	YBa_2InTe_5	*Cmc*2$_1$	[YTe_6]+[$InTe_4$]	2.40	34
48	Sc_2S_3	*Pnm*2$_1$	[ScS_8]+[ScS_6]	2.41	35
49	Gd_4GaSbS_9	*Aba*2	[GdS_7]+[GdS_6]+[GaS_4]+[SbS_4]	2.41	19
50	$YCuS_2$	*P*2$_1$2$_1$2$_1$	[YS_6]+[CuS_4]	2.46	36
51	$KTbP_2Se_6$	*P*2$_1$	[$TbSe_7$]+[P_2Se_6]	2.46	11
52	La_3LiGeS_7	*P*6$_3$	[LaS_8]+[LiS_4]+[GeS_4]	2.46	37
53	$LaKGeSe_4$	*P*2$_1$	[$LaSe_7$]+[$GeSe_4$]	2.47	38
54	$EuCdGeS_4$	*Ama*2	[EuS_8]+[CdS_4]+[GeS_4]	2.50	26
55	$KGdP_2Se_6$	*P*2$_1$	[GdS_7]+[P_2Se_6]	2.53	11
56	La_3AgSnS_7	*P*6$_3$	[LaS_8]+[AgS_3]+[SnS_4]	2.54	39
57	$La_6Ga_2GeS_{14}$	*P*6$_3$	[LaS_8]+[$Ga_{0.5}S_3$]+[Ga/GeS_4]	2.54	40
58	$Eu_2P_2S_6$	*Pn*	[EuS_8]+[P_2S_6]	2.54	42
59	La_3CuGeS_7	*P*6$_3$	[LaS_8]+[CuS_3]+[SiS_4]	2.57	42
60	Y_3GaS_6	*Cmc*2$_1$	[YS_8]+[GaS_4]	2.60	43
61	La_3LiSnS_7	*P*6$_3$	[LaS_j]+[SnS_4]	2.60	42
62	Y_3CuSnS_7	*P*6$_3$	[YS_7]+[CuS_3]+[SnS_4]	2.61	44
63	$La_6In_2GeS_{14}$	*P*6$_3$	[LaS_8]+[$In_{0.5}S_3$]+[In/GeS_4]	2.64	40
64	$LaScS_3$	*Pnm*2$_1$	[LaS_8]+[ScS_6]	2.65	45
65	$YScS_3$	*Pnm*2$_1$	[LaS_8]+[ScS_6]	2.65	46
66	$Ca_2CeBSiS_7$	*P*6$_3$mc	[Ca/CeS_6]+[BS_3]+[SiS_4]	2.65	47
67	Gd_3CuGeS_7	*P*6$_3$	[GdS_8]+[CuS_3]+[GeS_4]	2.67	42
68	$LiCeGeS_4$	*Ama*2	[$CeSe_8$]+[$LiSe_4$]+[$GeSe_4$]	2.72	48

69	$LaKSiSe_4$	$P2_1$	$[LaSe_7]+[SiSe_4]$	2.76	38
70	$Ba_4Sm_2Cd_3S_{10}$	$Cmc2_1$	$[SmS_8]+[SmS_7]+[CdS_4]$	2.77	49
71	$La_2Ga_2GeS_8$	$Cmc2_1$	$[LaS_8]+[GaS_4]+[GeS_4]$	2.78	28
72	Y_3NaSiS_7	$P6_3$	$[YS_7]+[SiS_4]$	2.80	50
73	Dy_3GaS_6	$Cmc2_1$	$[DyS_8]+[GaS_4]$	2.81	51
74	$LiSm_3SiS_7$	$P6_3$	$[SmS_8]+[LiS_4]+[SiS_4]$	2.83	52
75	$Y_4Si_3S_{12}$	$R3c$	$[YS_6]+[YS_7]+[SiS_4]$	2.87	56
76	$LiCeSiS_4$	$Ama2$	$[CeS_8]+[LiS_4]+[SiS_4]$	2.92	56
77	$LaSrGa_3S_7$	$P\bar{4}2_1m$	$[LaS_8]+[GaS_4]$	2.92	54
78	Y_3LiGeS_7	$P6_3$	$[YS_7]+[GeS_4]$	2.92	55
79	$ScLiS_2$	$R\bar{3}m$	$[ScS_6]+[LiS_6]$	2.94	56
80	$LaGaS_3$	$Pnm2_1$	$[LaS_8]+[GaS_4]$	2.94	57
81	$LaCaGa_3S_7$	$P\bar{4}21m$	$[La/CaS_8]+[GaS_4]$	2.96	58
82	La_3AlCdS_7	$P6_3$	$[LaS_8]+[AlS_4]+[CdS_6]$	2.98	59
83	La_3LiGeS_7	$P6_3$	$[LaS_8]+[LiS_4]+[GeS_4]$	3.02	37
84	Ho_3GaS_6	$Cmc2_1$	$[HoS_7]+[GaS_4]$	3.03	60
85	Er_3GaS_6	$Cmc2_1$	$[ErS_7]+[GaS_4]$	3.08	60
86	$La_4Ge_3S_{12}$	$R3c$	$[LaS_6] + [LaS_7] + [GeS_4]$	3.10	61
87	La_3AlMgS_7	$P6_3$	$[LaS_8] +[AlS_4]$	3.11	59
88	$LaBS_3$	$Pna2_1$	$[LaS_9]+[BS_3]$	3.18	62
89	$Ca_2GdBSiS_7$	$P6_3mc$	$[GdS_7]+[BS_3]+[SiS_4]$	3.20	47
90	$LiPrGeS_4$	$P6_3$	$[PrS_8]+[LiS_4]+[SiS_4]$	3.21	48
91	$LiNdGeS_4$	$P6_3$	$[NdS_8]+[LiS_4]+[SiS_4]$	3.22	48
92	$LaBS_3$	$Pna2_1$	$[LaS_9]+[BS_3]$	3.29	63
93	$LaKSiS_4$	$P2_1$	$[LaS_7]+[SiS_4]$	3.31	64
94	$LiLaGeS_4$	$P6_3$	$[LaS_8]+[LiS_6]+[GeS_4]$	3.32	48
95	$LaLiSiS_4$	$Ama2$	$[LaS_8]+[LiS_4]+[SiS_4]$	3.32	53
96	$YKGeS_4$	$P2_1$	$[YS_7]+[GeS_4]$	3.34	65
97	$Ca_2LaBSiS_7$	$P6_3mc$	$[LaS_7]+[BS_3]+[SiS_4]$	3.38	47
98	$CsSmSiS_4$	$P2_12_12_1$	$[SmS_7]+[SiS_4]$	3.51	This work
99	$YKSiS_4$	$P2_1$	$[YS_7]+[SiS_4]$	3.58	38
100	$CsLaGeS_4$	$P2_12_12_1$	$[LaS_7]+[SiS_4]$	3.60	66
101	$LiLaSiS_4$	$Ama2$	$[LaS_8]+[LiS_4]+[SiS_4]$	3.71	64
102	$CsGdSiS_4$	$P2_12_12_1$	$[GdS_7]+[SiS_4]$	3.72	This work
103	$LaCaAl_3S_7$	$P\bar{4}2_1m$	$[La/CaS_8]+[AlS_4]$	3.76	67
104	$CsTbSiS_4$	$P2_12_12_1$	$[TbS_7]+[SiS_4]$	3.76	This work

105	$LaSrAl_3S_7$	$P\bar{4}2_1m$	$[La/SrS_8]+[AlS_4]$	3.78	67
106	$CsDySiS_4$	$P2_12_12_1$	$[DyS_7]+[SiS_4]$	3.78	This work
107	$CsHoSiS_4$	$P2_12_12_1$	$[HoS_7]+[SiS_4]$	3.95	This work

Table S7 Measured LIDTs of **1**−**5** and AGS for their single-crystal samples.

Compound	Damage energy (mJ)	Spot area (cm^2)	Damage threshold (MW/cm^2)	Relative value
1	5.6	0.0254469	22.00660942	3.7
2	5.4	0.0254469	21.22065908	3.6
3	5.5	0.0254469	21.61363425	3.7
4	5.9	0.0254469	23.18553492	3.9
5	8.3	0.0254469	32.61693895	5.5
AGS	1.5	0.0254469	5.894627522	1

Table S8 Dipole moment within one-unit cell calculation results for **1**−**5**.

Compound		Dipole moment				
					Magnitude	
		x	*y*	*z*	Debye	× 10^{-4} esu·cm·Å^{-3}
1	SmS_7	-40.63	19.87	-35.35	57.40	0.30
	SiS_4	13.49	-34.10	1.68	36.71	0.19
	Unit cell	-27.49	-14.23	-33.68	45.53	0.24
2	GdS_7	67.34	3.61	19.49	70.19	0.37
	SiS_4	-25.40	-0.35	23.97	34.93	0.19
	Unit cell	41.94	3.26	43.46	60.48	0.32
3	TbS_7	64.58	2.81	17.88	67.06	0.36
	SiS_4	-25.19	-0.45	23.37	34.37	0.18
	Unit cell	39.39	2.35	41.25	57.08	0.30
4	DyS_7	64.42	3.83	16.69	66.65	0.36
	SiS_4	-25.09	-0.39	23.44	34.33	0.19
	Unit cell	39.33	3.44	40.13	56.29	0.30
5	HoS_7	62.97	2.93	17.70	65.84	0.35
	SiS_4	-25.40	-0.35	23.97	34.22	0.19
	Unit cell	37.57	2.58	41.67	56.17	0.30

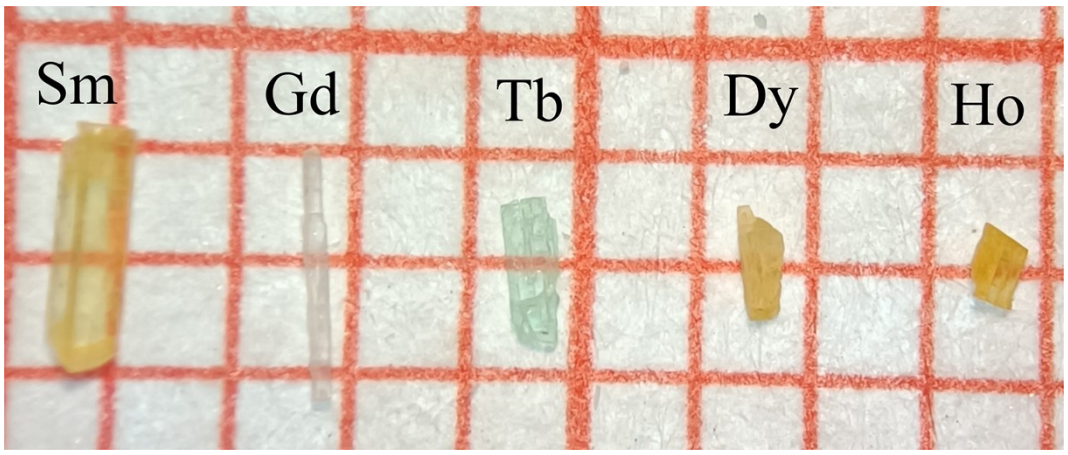

Figure S1 The crystals' photographs of **1**−**5**.

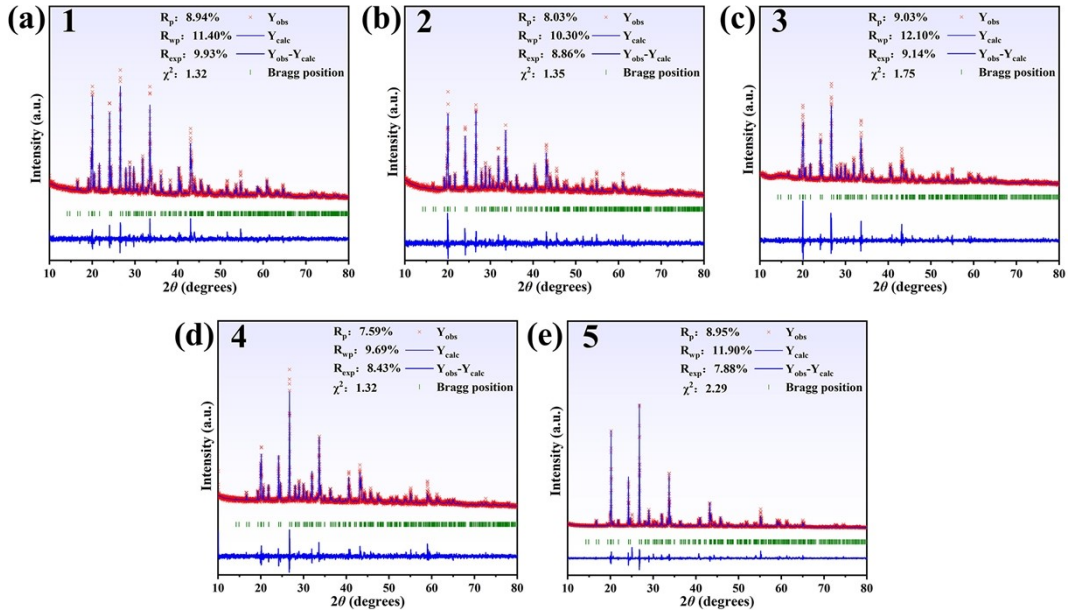

Figure S2 PXRD patterns of **1**−**5**.

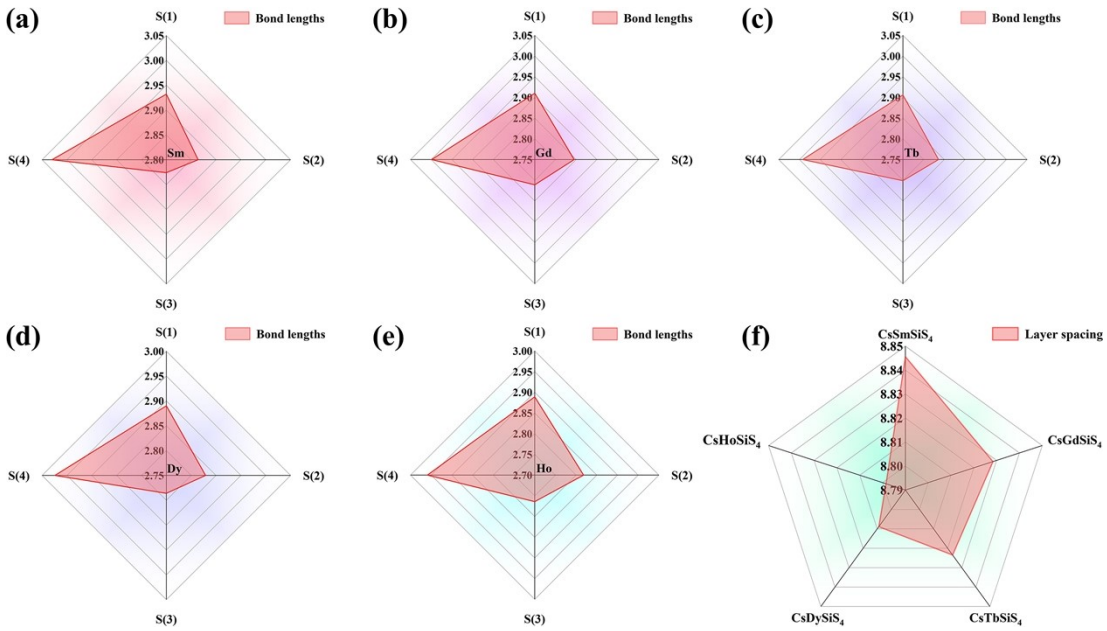

Figure S3 (a-e) The largest RE−S bond lengths in **1**−**5**; (f) layer spacing in the structures of **1**−**5**.

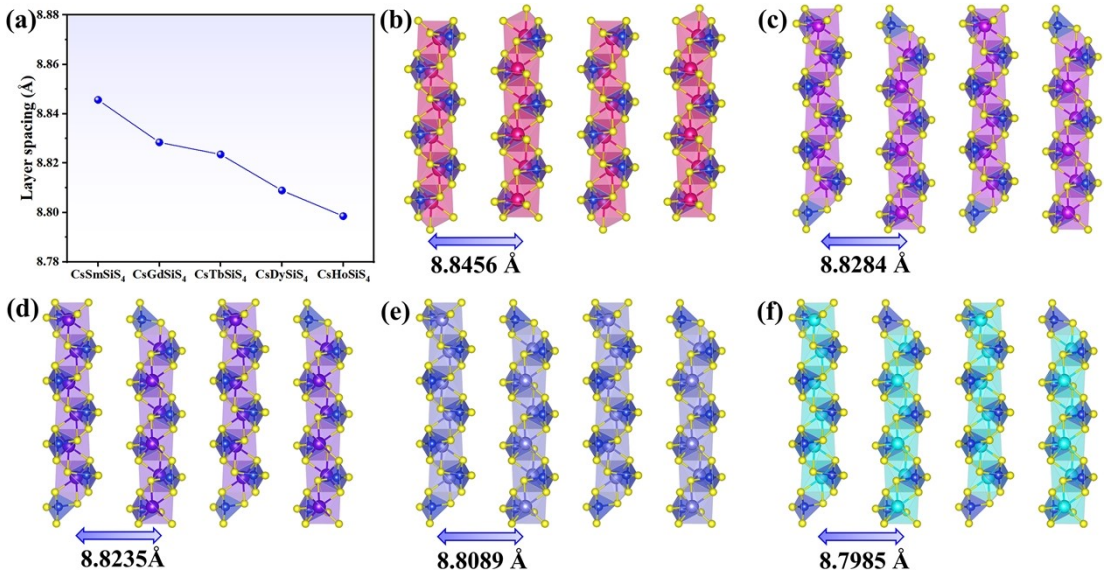

Figure S4 (a) The relationship between rare-earth element and layer spacing **1**−**5**; (b-f) the distances between $\{[GdSiS_5]^{3-}\}_n$ layers for **1**−**5**.

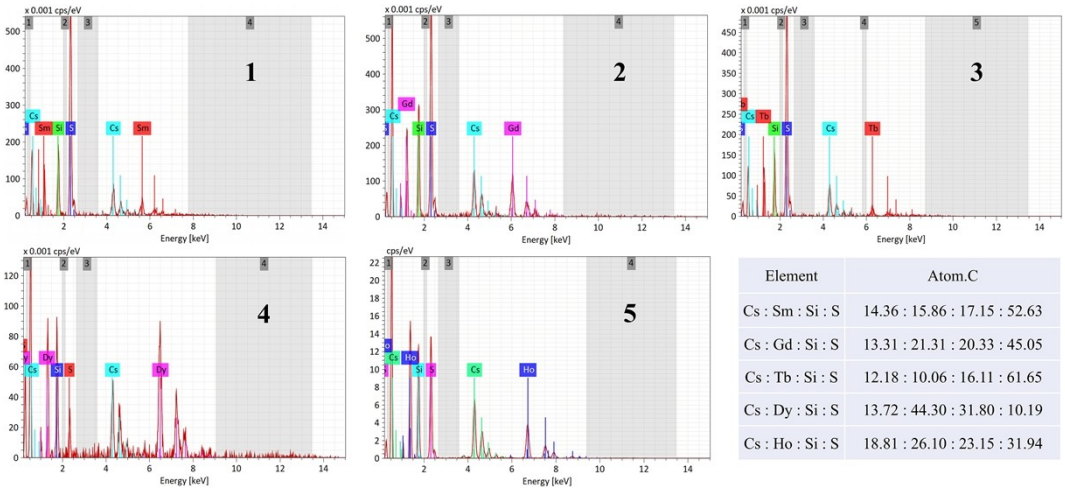

Element	Atom.C
Cs : Sm : Si : S	14.36 : 15.86 : 17.15 : 52.63
Cs : Gd : Si : S	13.31 : 21.31 : 20.33 : 45.05
Cs : Tb : Si : S	12.18 : 10.06 : 16.11 : 61.65
Cs : Dy : Si : S	13.72 : 44.30 : 31.80 : 10.19
Cs : Ho : Si : S	18.81 : 26.10 : 23.15 : 31.94

Figure S5 Energy dispersion spectroscopies of **1**−**5**.

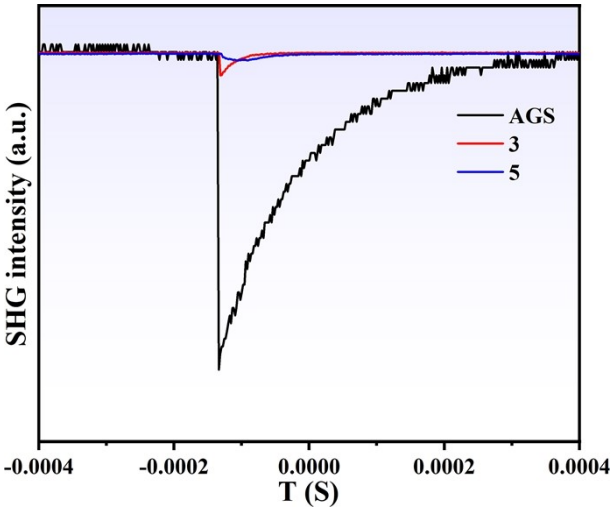

Figure S6 SHG intensities of **3**, **5** and AGS at 2.1 *μ*m for their 200−250 *μ*m samples.

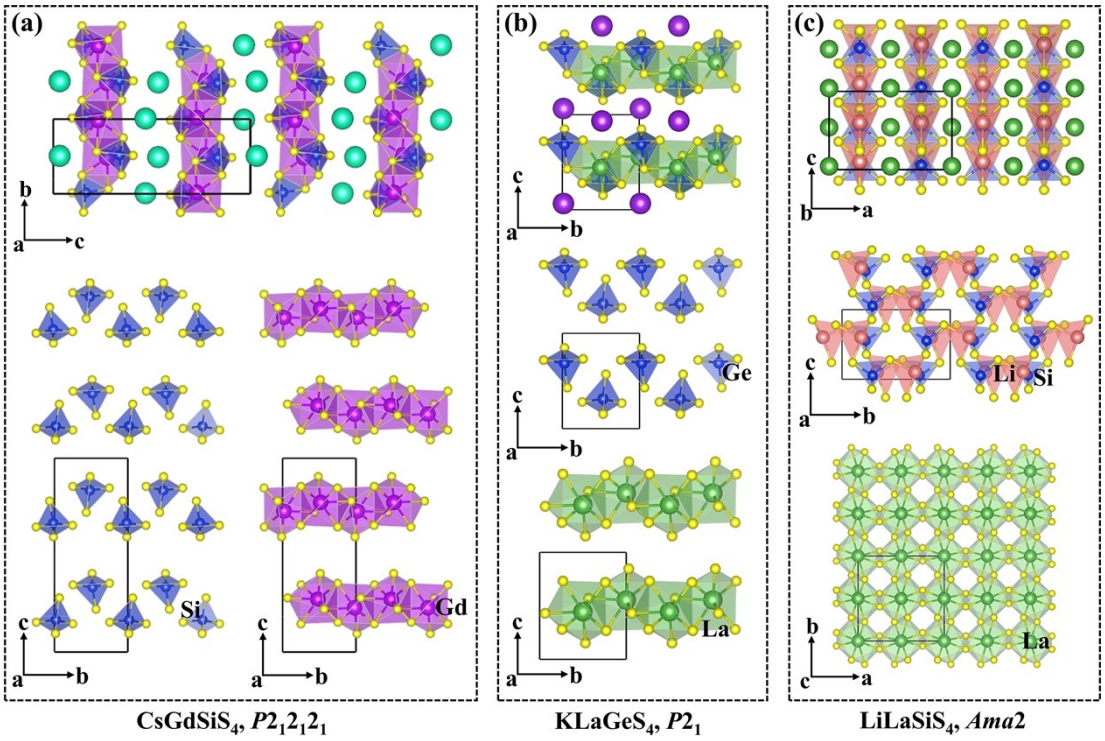

Figure S7 The structures of (a) $CsGdSiS_4$, (b) $KLaGeS_4$ and (c) $LiLaSiS_4$.

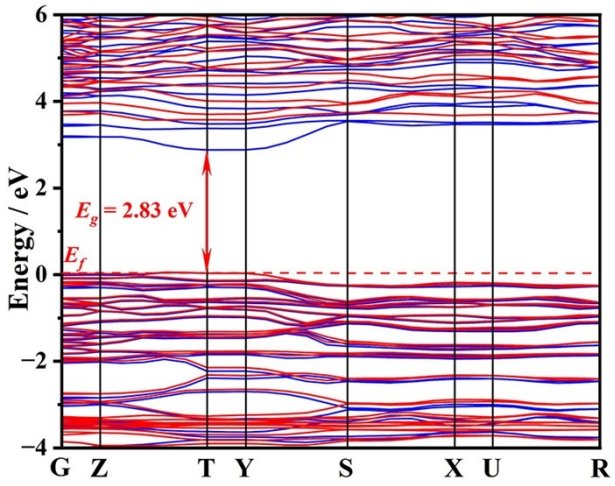

Figure S8 Band gap of **5**.

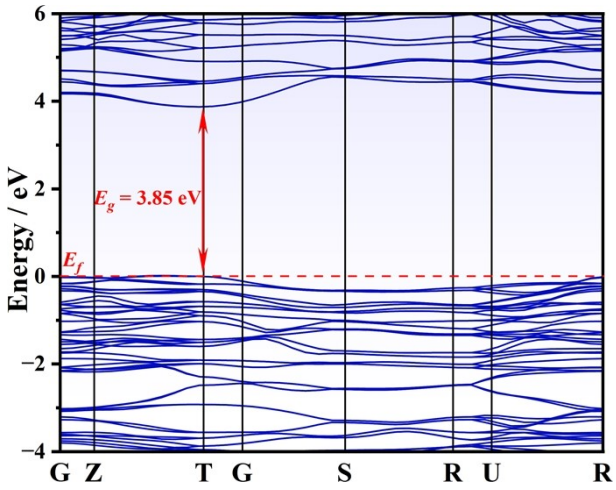

Figure S9 HSE06 band gap of **2**.

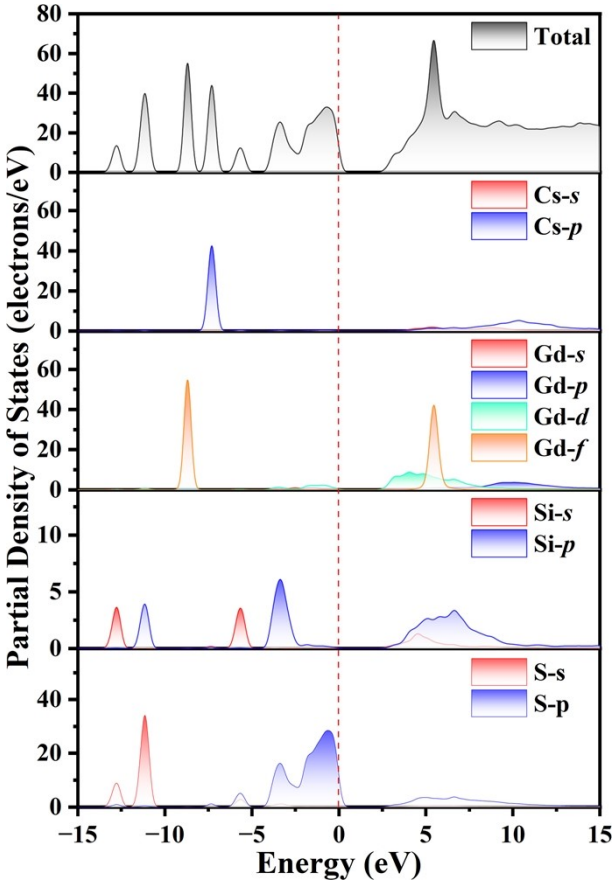

Figure S10 Partial density of states of **2**.

References

[1] Yin, W. L.; Wang, W. D.; Bai, L.; Feng, K.; Shi, Y. G.; Hao, W. Y.; Yao, J. Y.; Wu, Y. C., Syntheses, structures, physical properties, and electronic structures of Ba_2MLnTe_5 (M = Ga and Ln = Sm, Gd, Dy, Er, Y; M = In and Ln = Ce, Nd, Sm, Gd, Dy, Er, Y), *Inorg. Chem.,* 2012, **51**, 11736-11744.

[2] Collin, G.; Flahaut, J., Sur plusieurs series de composes non lacunaires de formule $L_6B_2C_2X_{14}$, *Bull. Soc. Chim Fr.,* 1972, **6**, 2207-2209.

[3] Deligoz, E.; Ozisik. H.; Ozisik, H. B., Prediction of new stable crystal structures for ternary $ErAgTe_2$ and $YAgTe_2$ semiconductors: Ab initio study, *Solid State Sci.,* 2023, **139**, 107160.

[4] Gulay, L. D.; Daszkiewicz. M.; Ruda, I. P.; Marchuk, O. V., La_2Pb $(SiS_4)_2$, *Acta Crystallogr. C,* 2010, **66**, i19-i21.

[5] Aliev, O. M., Some General Features of Reactions Between Chalcogenides of Elements of Subgroups IIIa and IIIb, *Inorg. Mater.,* 1981, **16**, 1027-1031.

[6] Xu, J. J.; Xiao, Y.; Wu, K.; Zhang, B. B.; Lu, D. Z.; Yu, H. H.; Zhang, H. J., Flexible Anionic Groups-Activated Structure Dissymmetry for Strong Nonlinearity in $Ln_2Ae_3M^{IV}_3S_{12}$ Family, *Small,* 2024, **20**, 2306577.

[7] Song, X. H.; Zhao, Y. C.; Ni, J.; Meng, S.; Dai, Z. H., High thermoelectric performance in $XAgSe_2$ (X = Sc, Y) from strong quartic anharmonicity and multi-valley band structure, *J. Mater. Chem. A,* 2023, **11**, 17138-17144.

[8] Hewage, N. W.; Viswanathan. G; Yox, P.; Wu, K.; Kovnir, K.; Akopov, G., Synthesis of chiral high-entropy sulfides for non-linear optical applications, *Inorg. Chem. Front.,* 2023, **10**, 6613-6621.

[9] Dismukes, J. P.; Smith, R. T.; White. J. G., Physical properties and crystal structure of a new semiconducting I-III-VI_2 compound, $CuScS_2$, *J. Phys. Chem. Solids,* 1971, **32**, 913-922.

[10] Zhao, H. J., Syntheses, crystal structures, and NLO properties of the quaternary sulfides $RE_3Sb_{0.33}SiS_7$ (RE = La, Pr), *J. Solid State Chem.,* 2015, **227**, 5-9.

[11] Chen, Z. X.; Zhao, C. Y.; Li, X. H.; Yao, W. D.; Liu, W. L.; Guo, S. P., $KREP_2Se_6$ (RE = Sm, Gd, Tb): The First Rare-Earth Selenophosphates with Remarkable Nonlinear Optical Activities Realized by Synergistic Effect of RE-and P-Based Motifs, *Small,* 2023, **19**, 2206910.

[12] Gulay, L. D.; Lychmanyuk, O. S.; Olekseyuk, I. D.; Daszkiewicz, M.; Stępień-Damm, J.; Pietraszko, A., Crystal structures of the compounds R_3CuSiS_7 (R = Ce, Pr, Nd, Sm, Tb, Dy and Er) and $R_3CuSiSe_7$ (R = La, Ce, Pr, Nd, Sm, Gd, Tb and Dy), *J. Alloys Compd.,* 2007, **431**, 185-190.

[13] Xing, W. H; Tang, C. L.; Wang, N. Z; Li, C. X.; Li, Z.; Wu, J. Y.; Lin, Z. S.; Yao, J. Y.; Yin, W. L.; Kang, B., $EuHgGeSe_4$ and $EuHgSnS_4$: two quaternary Eu-based infrared nonlinear optical materials with strong second-harmonic-generation responses, *Inorg. Chem.,* 2020, **59**, 18452-18460.

[14] Gulay, L. D.; Lychmanyuk, O. S.; Stępień-Damm, J.; Pietraszko, A.; Olekseyuk, I. D., Crystal structures of the Y_3CuSiS_7 and $Y_3CuSiSe_7$ compounds, *J. Alloys Compd.,* 2005, **402**, 201-203.

[15] Zhao, H. J.; Zhong, X. A., Synthesis, crystal structure, and optical properties of the noncentrosymmetric sulfide $Ce_8Sb_2S_{15}$, *J. Solid State Chem.,* 2017, **251**, 65-69.

[16] Gulay, L. D.; Olekseyuk, I. D., Crystal structures of the $R_3CuSnSe_7$ (R = La, Ce, Pr, Nd, Sm, Gd, Tb and Dy) compounds, *J. Alloys Compd.,* 2005, **388**, 274-278.

[17] Yan, M.; Sun, Z. D.; Yao, W. D.; Zhou, W. F.; Liu, W. L.; Guo, S. P., A highly distorted HgS_4 tetrahedron-induced moderate second-harmonic generation response of $EuHgGeS_4$, *Inorg. Chem. Front.,* 2020, **7**, 2451-2458.

[18] Lin, H.; Li, Y. Y.; Li, M. Y.; Ma, Z. J.; Wu, L. M.; Wu, X. T.; Zhu, Q. L., Centric-to-acentric structure transformation induced by a stereochemically active lone pair: a new insight for design of IR nonlinear optical materials, *J. Mater. Chem. C,* 2019, **7**, 4638-4643.

[19] Zhao, H. J.; Zhang, Y. F.; Chen, L., Strong Kleinman-forbidden second harmonic generation in chiral sulfide: La_4InSbS_9, *J. Am. Chem. Soc.,* 2012, **134**, 1993-1995.

[20] Daszkiewicz, M.; Gulay, L. D.; Pietraszko, A.; Shemet, V. Ya., Crystal structures of the $La_3AgSnSe_7$ and $R_3Ag_{1-\delta}SnS_7$ (R = La, Ce; δ = 0.18−0.19) compounds, *J. Solid State Chem.,* 2007, **180**, 2053-2060.

[21] Gulay, L. D.; Lychmanyuk, O. S.; Stępień-Damm, J.; Pietraszko, A.; Olekseyuk, I. D., Isothermal section of the Y_2S_3–Cu_2S–GeS_2 system at 870 K and crystal structures of the $Y_3Ge_{1.25}S_7$ and Y_3CuGeS_7 compounds, *J. Alloys Compd.,* 2006, **414**, 113-117.

[22] Zhao, H. J., Synthesis, crystal structure, and NLO property of the chiral sulfide Sm_4InSbS_9, *Z. Anorg. Allg. Chem.,* 2016, **642**, 56-59.

[23] Craig, A. J.; Cho, J. B.; Shin, S. H.; Ha, S. H.; Stoyko, S. S.; Jang, J. I.; Aitken, J. A., Homovalent cation substitutions leading to new lithium-containing La_3CuSiS_7 family members having chiral, uniaxial structures and exhibiting second-and third-harmonic generation, *J. Alloys Compd.,* 2022, **910**, 164855.

[24] Lychmanyuk, O.; Gulay, L.; Olekseyuk, I., Isothermal section of the Y_2Se_3-Cu_2Se-$GeSe_2$ system at 870 K and crystal structure of the $Y_3CuGeSe_7$ compound, *Pol. J. Chem.,* 2006, **80**, 463-469.

[25] Chen, M. C.; Li, L. H.; Chen, Y. B.; Chen, L., In-phase alignments of asymmetric building units in Ln_4GaSbS_9 (Ln = Pr, Nd, Sm, Gd− Ho) and their strong nonlinear optical responses in middle IR, *J. Am. Chem. Soc.,* 2011, **133**, 4617-4624.

[26] Xing, W. H.; Wang, N. Z; Guo, Y. W.; Li, Z.; Tang, J. Kang, K. J.; Yin, W. L.; Lin, Z. S.; Yao, J. Y.; Kang, B., Two rare-earth-based quaternary chalcogenides $EuCdGeQ_4$ (Q= S, Se) with strong second-harmonic generation, *Dalton Trans.,* 2019, **48,** 17620-17625.

[27] Strok, O. M.; Daszkiewicz, M.; Gulay, L. D.; Kaczorowski, D., Crystal structure and magnetic properties of Sm_3CuGeS_7 and $Sm_3CuGeSe_7$, *J. Alloys Compd.,* 2010, **493**, 47-49.

[28] Chen, M. C.; Li, P.; Zhou, L. J.; Li, L. H.; Chen, L., Structure change induced by terminal sulfur in noncentrosymmetric $La_2Ga_2GeS_8$ and $Eu_2Ga_2GeS_7$ and nonlinear-optical responses in middle infrared, *Inorg. Chem.,* 2011, **50**, 12402-12404.

[29] Zhao, H. J.; Zhou, L. J., A Series of Noncentrosymmetric Antimony Sulfides $Ln_8Sb_2S_{15}$ (Ln = La, Pr, Nd)–Syntheses, Crystal and Electronic Structures, and NLO Properties, *Eur. J. Inorg. Chem.,* 2015, **6**, 964-968.

[30] Azam, S.; Gul, B.; Ali, N.; Ahmad, K.; Khan, R.; Hegazy, H. H.; Khan, W.; Aftab, S.; Rahman, A. U., Enlightening the stability and optoelectronic properties of

Ba_2MLnSe_5 (M = Ga, In; Ln = Y, Nd, Sm, Gd, Dy, Er) semiconductors: A first-principles study, *J. Solid State Chem.,* 2023, **319**, 123767.

[31] Gulay, L. D.; Olekseyuk, I. D.; Wołcyrz, M.; Stępień-Damm, J., The Crystal Structures of R_3CuSnS_7 (R = La–Nd, Sm, Gd–Ho), *Z. Anorg. Allg. Chem.,* 2005, **631**, 1919-1923.

[32] Wu, L. B.; Huang, F. Q., Crystal structure of trilanthanum monosilver monosilicon heptasulfide, La_3AgSiS_7, *Z. Krist.-New Cryst. Struct.,* 2005, **220**, 327-328.

[33] Hwu, S. J.; Bucher, C. K.; Carpenter, J. D.; Taylor, S. P., A solid-state diastereomer, $AgLa_3GeS_7$, *Inorg. Chem.,* 1995, **34**, 1979-1980.

[34] Yin, W. L.; Wang, W. D.; Bai, L.; Feng, K.; Shi, Y. G.; Hao, W. Y.; Yao, J. Y.; Wu, Y. C., Syntheses, structures, physical properties, and electronic structures of Ba_2MLnTe_5 (M = Ga and Ln = Sm, Gd, Dy, Er, Y; M = In and Ln = Ce, Nd, Sm, Gd, Dy, Er, Y), *Inorg. Chem.,* 2012, **51**, 11736-11744.

[35] Azarapin, N. O.; Oreshonkov, A. S.; Razumkova, I. A.; Aleksandrovsky, A. S.; Maximov, N. G.; Leonidov, I. I.; Shestakov, N. P.; Andreev, O. V., Evolution of Structural, Thermal, Optical, and Vibrational Properties of Sc_2S_3, $ScCuS_2$, and $BaScCuS_3$ Semiconductors, *Eur. J. Inorg. Chem.,* 2021, **33**, 3355-3366.

[36] Baghdad, A. H.; Bouafia, H.; Djebour, B.; Sahli, B; Hiadsi, S.; Elchikh, M.; Attou, M., Study of phase transitions and lattice dynamics, elastic and electronic properties, bonding and weak interactions analysis of $YCuS_2$ in $P2_12_12_1$, $I\bar{4}2d$ and $P\bar{4}2_1m$ space group structures, *J. Phys. Chem. Solids,* 2022, **167**, 110756.

[37] Yang, Y.; Chu, Y.; Zhang, B. B.; Wu, K.; Pan, S. L., Unique unilateral-chelated mode-induced d–p–π interaction enhances second-harmonic generation response in new Ln_3LiMS_7 family, *Chem. Mater.,* 2021, **33**, 4225-4230.

[38] Wu, P.; Ibers, J. A., Synthesis and structures of the quaternary chalcogenides of the type $KLnMQ_4$ (Ln = La, Nd, Gd, Y; M = Si, Ge; Q= S, Se), *J. Solid State Chem.,* 1993, **107**, 347-355.

[39] Zeng, H. Y.; Zheng, F. K.; Guo, G. C.; Huang, J. S., Syntheses and single-crystal structures of La_3AgSnS_7, $Ln_3M_xMS_7$ (Ln = La, Ho, Er; M = Ge, Sn; $1/4 \leq x \leq 1/2$), *J. Alloys Compd.,* 2008, **458**, 123-129.

[40] Shi, Y. F.; Chen, Y. K.; Chen, M. C.; Wu, L. M.; Lin, H.; Zhou, L. J.; Chen, L., Strongest second harmonic generation in the polar R_3MTQ_7 family: atomic distribution induced nonlinear optical cooperation, *Chem. Mater.,* 2015, **27**, 1876-1884.

[41] Huang, X.; Yang, S. H.; Li, X. H.; Liu, W. L.; Guo, S. P., $Eu_2P_2S_6$: The First Rare-Earth Chalcogenophosphate Exhibiting Large Second-Harmonic Generation Response and High Laser-Induced Damage Threshold, *Angew. Chem. Int. Ed.,* 2022, **61**, e202206791.

[42] Akopov, G.; Hewage, N. W.; Viswanathan, G.; Yox, P.; Wu, K.; Kovnir, K., Non-Linear Optical Properties of the $(RE)_3CuGeS_7$ Family of Compounds, *Z. Anorg. Allg. Chem.,* 2022, **648**, e202200096.

[43] Zhang, M. J.; Li, B. X.; Liu, B. W.; Fan, Y. H.; Li, X. G.; Zeng, H. Y.; Guo, G. C., Ln_3GaS_6 (Ln = Dy, Y): new infrared nonlinear optical materials with high laser induced damage thresholds, *Dalton Trans.,* 2013, **42**, 14223-14229.

[44] Gulay, L. D.; Shemet, V. Y.; Olekseyuk, I. D., Crystal structures of the compounds $YCuS_2$, Y_3CuSnS_7 and $YCuPbS_3$, *J. Alloys Compd.,* 2005, **388**, 59-64.

[45] Zhang, H.; Pan, Y. C.; Liu, Z. X.; Zeng, B. Wu, X. W.; Ming, C.; Xin, G. Q.; Zhou, W. H.; Zeng, H.; Zhang, S. B.; Sun, Y. Y., Indirect-to-direct band gap transition induced by d-d coupling between cations in rare-earth chalcogenide perovskites, *Phys. Rev. B,* 2024, **110**, L041201.

[46] Carré, D.; Flahaut, J.; Khodadad, P.; Laruelle, P.; Rodier, N.; Tien, V. V., Etude comparée des structures cristallines des sulfures contenant deux eléments IIIA (scandium, yttrium et lanthanides), *J. Solid State Chem.,* 1973, **7**, 321-336.

[47] Han, Y. X.; Hu, C. L.; Mao, J. G., $Ca_2Ln(BS_3)(SiS_4)$ (Ln = La, Ce, and Gd): Mixed Metal Thioborate-Thiosilicates as Well-Performed Infrared Nonlinear Optical Materials, *Small,* 2024, **20**, 2305828.

[48] Liu, Q. Q.; Liu, X.; Li, M. Z.; Wang, R. X.; Li, B. X.; Wu, L. M.; Chen, Lin., $LiLnGeS_4$ (Ln = La−Nd): Designing High Performance Infrared Nonlinear Optical Sulfides through "Band Reformation of AGS"*, Angew. Chem. Int. Ed.,* 2025, **64**, e202415318.

[49] Yue, Q. G.; Zhou, S. H.; Li, B. X.; Wu, X. Y.; Lin, H.; Zhu, Q. L., Quaternary Noncentrosymmetric Rare-Earth Sulfides $Ba_4RE_2Cd_3S_{10}$ (RE = Sm, Gd, or Tb): A Joint Experimental and Theoretical Investigation*, Inorg. Chem,* 2022, **61**, 1797-1804.

[50] Hartenbach, I.; Schleid, T., $NaY_3S_3[SiS_4]$: a sodium-containing yttrium sulfide thiosilicate with channel structure*, J. Solid State Chem.,* 2003, **171**, 382-386.

[51] Zhen, N.; Nian, L. Y.; Li, G. M.; Wu, K.; Pan, S. L., A high laser damage threshold and a good second-harmonic generation response in a new infrared NLO material: $LiSm_3SiS_7$, *Crystals,* 2016, **6**, 121.

[52] Bardelli, S.; Ye, Z. Y.; Wang, F.; Zhang, B. B.; Wang, Jian., Synthesis, Crystal and Electronic Structures, and Nonlinear Optical Properties of $Y_4Si_3S_{12}$, *Z. Anorg. Allg. Chem.,* 2022, **648**, e202100388.

[53] Han, Y. X.; Hu, C. L.; Li, B. X.; Mao, J. G., $LnLiSiS_4$ (Ln= La and Ce): Promising infrared nonlinear optical materials designed by aliovalent substitution from $SrCdSiS_4$, *Mater. Today Phys.,* 2023, **31**, 100987.

[54] Xu, J. J.; Wu, K.; Xiao, Y.; Zhang, B. B.; Yu, H. H.; Zhang, H. J., Mixed-anion-oriented design of $LnMGa_3S_6O$ (Ln = La, Pr, and Nd; M = Ca and Sr) nonlinear optical oxysulfides with targeted property balance, *ACS Appl. Mater. Interfaces,* 2022, **14**, 37967-37974.

[55] Gao, L. H.; Wu, X. W.; Xu, J. J.; Tian, X. Y.; Zhang, B. B.; Wu, K., Rational combination of multiple structural groups on regulating nonlinear optical property in hexagonal Ln_3MGeS_7 polar crystals, *J. Alloys Compd.,* 2022, **900**, 163535.

[56] Van Dijk, M.; Plug, C. M., The crystal structure of $LiScS_2$ and $NaScS_2$. *Mater. Res. Bull.,* 1980, **15**, 103-106.

[57] Li, P.; Li, L. H.; Chen, L. Wu, L. M., Synthesis, structure and theoretical studies of a new ternary non-centrosymmetric *β*-$LaGaS_3$, *J. Solid State Chem.,* 2010, **183**, 444-450.

[58] Mazurier, A.; Jaulmes, S.; Guittard, M., Structure cristalline dun nouveau composé isotype de la mélilite, $Ca_2La_2Ga_6S_{14}$, *Acta. Crystallogr. C,* 1987, **43**, 1859-1861.

[59] Collin, G.; Flahaut, J., Sur une famille de composes de type $La_6Mn_2Al_2S_{14}$, CR *Acad. Sci., Ser. C,* 1970, **270**, 488-490.

[60] Chen, H. Y.; Zhang, Y. Y.; Yang, Y. F.; Guo, S. P., Ternary rare-earth sulfides RE_3GaS_6 (RE= Ho, Er): Crystal chemistry, second-order nonlinear optical properties and theoretical investigation, *J. Alloys Compd.,* 2021, **868**, 159112.

[61] Cicirello, G.; Wu, K.; Zhang, B. B.; Wang, J., Applying band gap engineering to tune the linear optical and nonlinear optical properties of noncentrosymmetric chalcogenides $La_4Ge_3SexS_{12-x}$ (x = 0, 2, 4, 6, 8, 10), *Inorg. Chem. Front.* 2021, **8**, 4914-4923.

[62] Han, Y. X.; Hu, C. L.; Fang, Z.; Chen, Q. Q.; Li, B. X.; Lin, Y.; Mao, J. G., $LaBS_3$ revisited: a promising mid-infrared nonlinear optical material, *J. Mater. Chem. C,* 2022, **10**, 12556-12559.

[63] Breton, L. S.; Morrison, G.; Lacroix, M. R.; Halasyamani, P. S.; Loye, H. C. Z., Lanthanide thioborates, an emerging class of nonlinear optical materials, efficiently synthesized using the boron–chalcogen mixture method, *Chem. Commun,* 2022, **58**, 7992-7995.

[64] Wang, H. S; Pan, X. T.; Pan, S. L.; Li, J. J., Chemical modulation of $A^{I}RE^{III}C^{IV}Q^{VI}_4$ family compounds for band gap and optical anisotropy enhancement, *Inorg. Chem. Front.,* 2024, **11**, 6919-6927.

[65] Mei, D. J.; Cao, W. Z.; Wang, N. Z.; Jiang, X. X.; Zhao, J.; Wang, W. K.; Dang, J. H.; Zhang, S. Y.; Wu, Y. D.; Rao, P. H.; Lin, Z. S., Breaking through the “3.0 eV wall” of energy band gap in mid-infrared nonlinear optical rare earth chalcogenides by charge-transfer engineering, *Mater. Horiz.,* 2021, **8**, 2330-2334.

[66] Usman, M.; Smith, M. D.; Morrison, G.; Klepov, V. V.; Zhang, W. G.; Halasyamani, P. S.; Loye, H. Z., Molten alkali halide flux growth of an extensive family of noncentrosymmetric rare earth sulfides: structure and magnetic and optical (SHG) properties, *Inorg. Chem.,* 2019, **58**, 8541-8550.

[67] Xu, J. J.; Wu, K.; Zhang, B. B.; Yu, H. H.; Zhang, H. J., $LaAeAl_3S_7$ (Ae = Ca, Sr): Cairo pentagonal layered thioaluminates achieving a good balance between a strong second harmonic generation response and a wide bandgap, *Inorg. Chem. Front.,* 2023, **10**, 2045-2052.